Development of Distributed Optical Torque Sensors for Realization of Local Impedance Control of the Robot Arm

Dzmitry Tsetserukou, Riichiro Tadakuma, Hiroyuki Kajimoto and Susumu Tachi
Graduate School of Information Science and Technology
The University of Tokyo
7-3-1 Hongo, Bunkyo-ku, Tokyo, 113-8656, Japan.
Email: dima_teterukov@ipc.i.u-tokyo.ac.jp

This paper describes the recent development of optical torque sensor in order to replace expensive strain gauge sensor attached at the tip of the anthropomorphic robot arm and realize local impedance control in each joint. Different shapes of mechanical structure of sensor as well as optical measurement approaches are given. The results of calculation of stress and tangential displacement using Finite Element Method and experimental results of research are presented. The concept of local impedance control of joints of humanoid robot arm is considered.

1. INTRODUCTION

The teleoperated slave robot has been developed to realize dexterous tasks as interaction with human in remote environment or manipulation with objects in hazardous conditions. The slave robot [1] includes anthropomorphic seven-degree of freedom (7-DOF) arms with 8-DOF hands (Fig. 1). To achieve the stability in contact with environment and to realize controlled dynamic interaction between a robot arm and human the impedance control has been successfully applied. The impedance control of the arm of the remote slave robot requires measurement of external force exerted by human during interaction [2]. The force imparted by human at the tip of the anthropomorphic arm is measured by 6-axes force sensor (MINI 4/20, made by BL AUTOTEC), marked by yellow rectangles in Fig. 1.

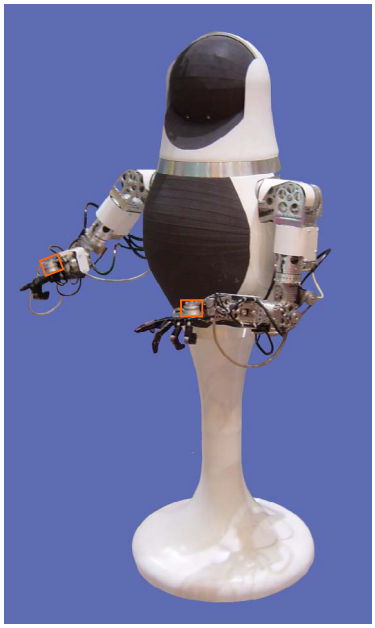

Fig. 1 Teleoperated slave robot

In spite of the fact that developed robotic system ensures the safety in the interaction at the end-effector, other parts of the mechanical structure, such as shoulder and elbow joint, during operation can hurt people. In these joints there are no force measurement sensors to limit the motor torque by means back loop. Direct sensing of applied torque through the value of current in DC motor circuit is unacceptable due to low backdrivability of harmonic drives with high gear ratio (=50). Therefore, to realize human friendly interaction of any part of the anthropomorphic arm we decided to attach torque sensor at each joint and, thus, to implement local impedance control. Thus, virtual backdrivability of transmissions can be achieved in each joint of slave robot.

Moreover, commercial force sensors using strain gauges typically measure all six axes - forces and torques – and intended for use at the end-effector of a robot to monitor assembly or machining forces. In this application very high stiffness is required. For human-robot interaction high stiffness is not the objective. Also strain gauges have many disadvantages. They are difficult to install, calibrate and easy to break that makes them expensive.

The authors introduce the idea of using optical approach to detect torque and realization of the local impedance control on the base of optical sensors to provide safety of interaction.

2. DEVELOPMENT OF THE OPTICAL TORQUE SENSOR

2.1 Optical Approaches of the Torque and Force Measurement

The idea of optical methods is non-contact measurement of relative twist or displacement of the components of the sensor caused by torque or force using photosensors. Photosensors have the similar drawbacks inherent to the strain gauges, such as nonlinearity and temperature sensitivity, but they are considerably more reliable, cheap and allow simplifying the construction of the design.

A significant contribution to research of the optical force and moment sensors was made by Shigeo Hirose [3, 4]. The author proposed to use a split type photosensor to detect the displacement of the light source caused by applied force. In the paper [5] authors used infrared LED-photodiode pairs to detect force. This optical force sensor consists of outer mount, inner part and flexure connected to the inner part. Optical sensors are attached to the inner part. The force applied to the inner part bend the flexure. Light from LED reflects the output piece and is detected by a photodiode. Thus, the distance between flexure and fixed part is measured and, hence, force can be calculated. The idea of the patent [6] is calculating torque

by measuring angle of twist of the torsion shaft through detection of difference in the rotation position of discs attached at the opposite sides of the torsion shaft using optical encoder. Structure of 6-axes force and torque converter using LEDs and photodiodes to detect bending is given in [7].

Drawbacks of above-mentioned optically based torque sensors are precise adjustment of the light source and detector position, complicated calibration procedure due to nonlinear output and large overall dimensions. To overcome main pointed disadvantages of the sensors and develop optical torque sensor as light as possible with compact size and high sensitivity we decided to use ultra-small size photointerrupters type RPI-131 and RPI-121. The relationship between output and position of the shield plate for RPI-121 is presented in Fig. 2 [8].

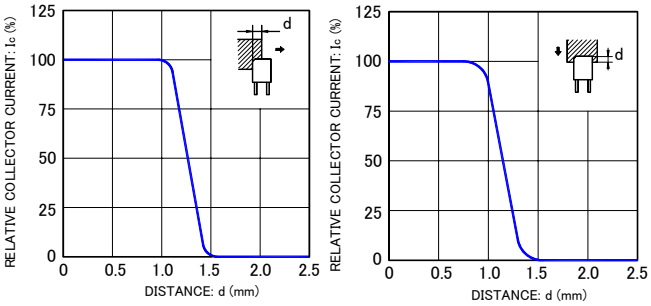

Fig. 2 Relative output vs. distance

For detecting of relative displacement of torque sensor components it is possible to use the linear section of diagram corresponding approximately 0.3 mm.

2.2 Analysis of Mechanical Structure. Determination of the Optimal Shape

To increase the signal-to-noise ratio of the sensor, it is desirable to design a structure that generates a large angle of twist for a given loading torque and, therefore, provides a high sensitivity. However, the resulting compliance introduces a joint angle error that should be minimized. Thus, one of the primary design trade-offs is between the stiffness and the sensitivity of the sensor.

The other difficulty in design of the torque sensor is eliminating hysteresis. Most metals used as flexures have very little hysteresis. However, bolted, press fit and welded joints near the flexure introduce hysteresis. Therefore, the optimal design requires realization of the mechanical structure of the sensor from a single piece of metal. It is also important to use differential measurements to increase the linearity and disturbance rejection of the torque sensors.

Taking into account above-mentioned, two main types of the mechanical structure were investigated: the “serial” structure – when the input and output section of the detector are displaced in axial direction by torsion component. And the “parallel” structure – when input and output of the sensor are disposed in one plane and linked by bending radial flexures.

The “serial” structure permits transmission of large torque under small outer diameter of the sensor. The main disadvantage is large overall length. Moreover, spring introduces considerable angle error caused significant compliance. In “parallel” structure the radial flexures are subjected by bending forces. The layout of widely used spoke structure of the hub having three flexures is presented in Fig. 3. Detector consists of input part, output part connected by flexure 1, fixedly mounted photointerrupters 2, shield 3. The operation principle is the following: when torque T is applied to the input shaft the flexures 1 will be deflected. This causes motion of the shield 3. The shield displacement is detected by the degree of interruption of infrared light falls on the phototransistor. Thus, magnitude of the output signal of photointerrupter will correspond to the applied torque.

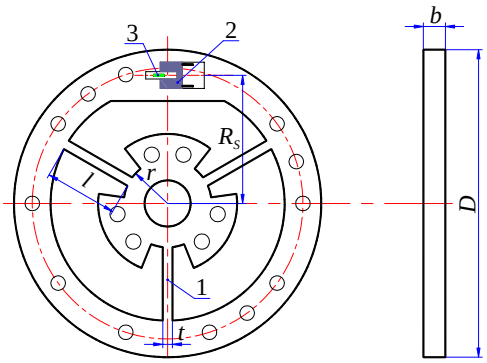

Fig. 3 Hub layout

The relationship between the sensed torque T_S and the angle of twist θ is following:

$$T_S = k_S\theta = k_S\left(\theta_1 - \theta_2\right) \tag{1}$$

where k_S – torsional stiffness of the cross-shaped spring.

The rigidity of the hub can be increased by introducing additional evenly distributed spokes [9]. The torsional stiffness of this sensor is derived from:

$$k_S = 4NEI\left(\frac{1}{l} + \frac{3r}{l^2} + \frac{3r^2}{l^3}\right) \tag{2}$$

where N – number of spokes, l – the spoke length, E – modulus of elasticity, r – inner radius of the sensor [10]. Moment of inertia of the spoke cross section I can be calculated as:

$$I = \frac{bt^3}{12}. \tag{3}$$

Here b – beam width, t – beam thickness. The sensor was designed to withstand torque of 0.8 Nm. The results of analysis using FEM show von Mises stress in MPa (Fig. 4a) and tangential displacement in mm (Fig. 4b) under torque of 0.8 Nm. The maximum value of von Mises stress equals $\sigma_{vonMises}$=14.57·10^7 N/m^2 <σ_{yield}=15.0·10^7 N/m^2). Angle of twist can be calculated from the value of tangential displacement.

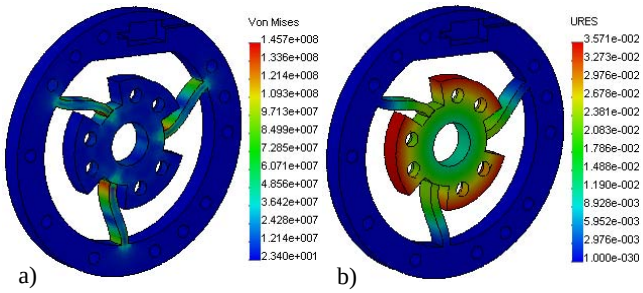

Fig. 4 FEM results

The test rig for calibration of the optical sensor has been created (Fig.5). Force applied to the arm secured by screw to the rotatable shaft creates the loading torque. Calibration was realized by means incrementation of angle of twist with small step and measuring output signal from the photointerrupter.

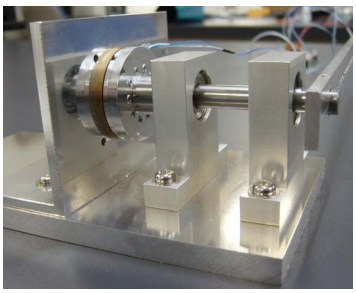

Fig. 5 Test rig

Obtained relationship between angle of twist and output voltage is shown in Fig. 6.

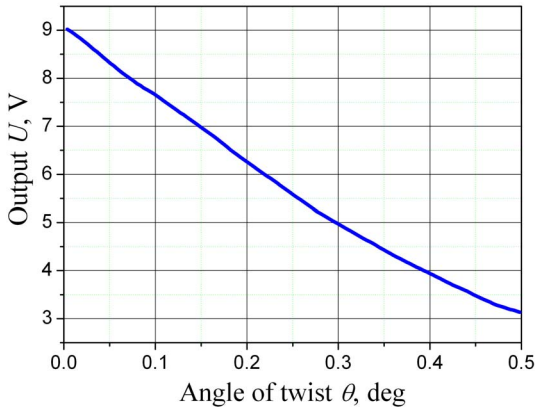

Fig. 6 Calibration result

The sensor was manufactured from one piece of brass by using wire electrical discharge machining that allowed to receive very precise dimensions of spokes (Fig.7).

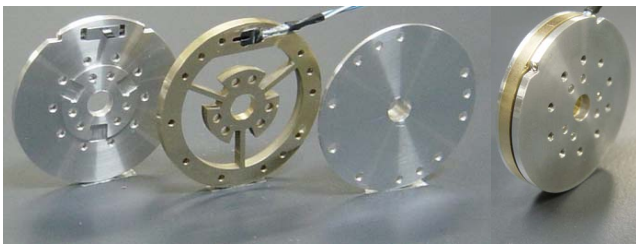

Fig. 7 Optical torque sensor with spoke topology

In this sensor the ultra-small photointerruptor RPI-121 is used. The thickness of the sensor body is only 6.5 mm. The adjustment of shield position is realized by rotation of screws. The pitch of the screws is enough for smoothly movement of slider with shield plate.

In order to improve the reliability of the mechanical structure of the transducer and enhance the flexibility the new topology of the sensor has been developed. Three-dimensional model and result of stress analysis are given in Fig. 8.

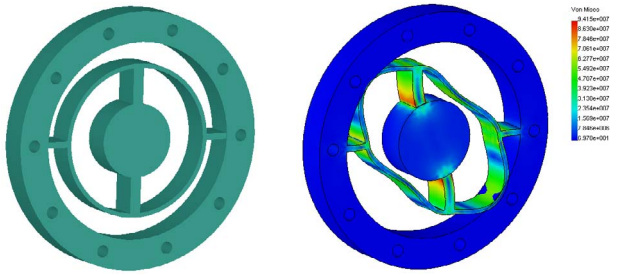

Fig. 8 New topology and its stress analysis

The flexible ring is connected with inner and outer part of the sensor though beams. The inner and outer beams are displaced with angle of 90° enabling large compliance of the ring-shaped flexure. For calibration of the senor the set up shown in Fig. 5 was utilized. Obtained relationship between angle of twist θ and the output voltage of photointerrupter is shown in Fig. 9.

Fig. 9 Calibration result

This structure was manufactured from one piece of aluminum. Components and assembly of the torque sensor with ring-shaped flexure are presented in Fig. 10.

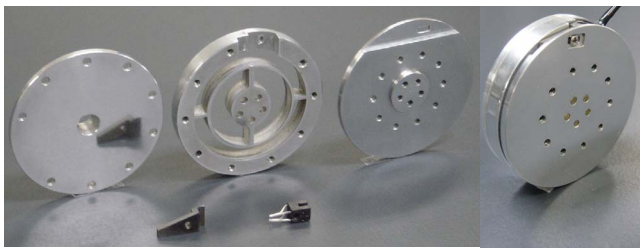

Fig. 10 Optical torque sensor with ring-shaped flexure

The thickness of the sensor is 10 mm. The displacement of the shield is measured by photointerruptor type RPI-131. Exploded three-dimensional view of the optical sensor is given in Fig. 11.

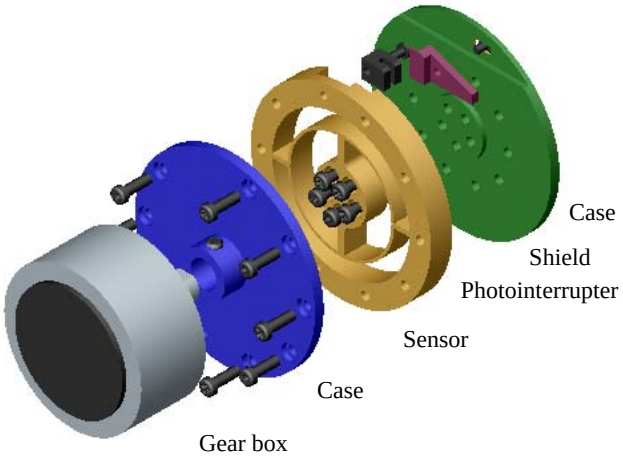

Fig. 11 Exploded view

The shortcomings of this design are complicated procedure of adjusting the position of the shield relatively photosensor and lack of the housing to prevent from damage of the optical transducer. Mechanical properties of the realized topologies of load cell are listed in Table 1.

Table 1 Mechanical properties

Type	Spoke- shaped flexure	Ring-shaped flexure
Material	Brass C2801	Aluminium A5052
Mass, g	18.52	9.2
Thickness/ Length, mm	3	5
Outer diameter, mm	42	42
Max. torque, Nm	0.8	0.8
Factor of safety	1.03	1.0
Torsional stiffness, Nm/rad	219.8	121.91

Considering obtained characteristics we can define advantages and shortcomings of the developed structures. Spoke-hub topology allows realization compact in axial direction sensor, however, big torsional stiffness diminishes the resolution of the photointerrupter. The ring-shaped flexure provides wide range of the torsional stiffness with high mechanical strength. To enlarge the allowable transmitted torque such material as spring steel or brass can be used.

2. LOCAL IMPEDANCE CONTROL

Dynamics of the manipulator during interaction with environment is described by the equation:

$$\tau + \tau_{EXT} = M(\Theta)\ddot{\Theta} + V(\Theta, \dot{\Theta}) + G(\Theta) \qquad (4)$$

Where τ – required torque from actuator to realize control law, τ_{EXT} – external torque applied from environment, $M(\Theta)$ – mass matrix, $V(\Theta, \dot{\Theta})$ – vector of centrifugal and Coriolis erms, $G(\Theta)$ – vector of gravity terms.

The aim of the impedance control is to establish the dynamic relationship between position error and force error in interaction similar to Newton`s second low of motion. The graphical presentation of concept of impedance control is given in Fig. 12.

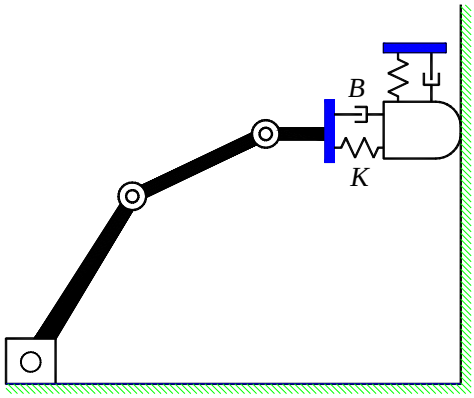

Fig. 12 Concept of the impedance control

In joint space system desired dynamics of joint *i* of robot arm is:

$$\tau_{iEXT} = M_d\ddot{\theta}_i + B_d\left(\dot{\theta}_i - \dot{\theta}_0\right) + K_d\left(\theta_i - \theta_0\right) \qquad (5)$$

Here M_d – desired inertia, B_d – desired viscousness, K_d – desired stiffness, θ_0 – desired joint angle, $\dot{\theta}_0$ – desired angular velocity of the joint, τ_{iEXT} – external torque applied to the joint *i*. The concept of local impedance control is presented in Fig. 13.

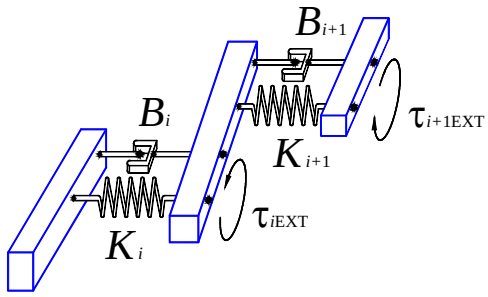

Fig. 13 Concept of local impedance control

In order to verify the dynamic behaviour of the optical torque sensor the torque control of three links of simple SCARA type manipulator has been developed. The control law of a PD controller is as follows [11]:

$$i\tau_m = \tau_d - K_P\left(\tau_S - \tau_d\right) - K_D\tau_S \qquad (6)$$

where i – gear ratio, τ_m – motor torque, K_P and K_D – proportional and derivative feedback gains respectively, τ_d – desirable torque, τ_S – sensed torque. Block diagram of PD torque control is presented in Fig. 14, the three links with driving motors and control circuits are shown in Fig. 15.

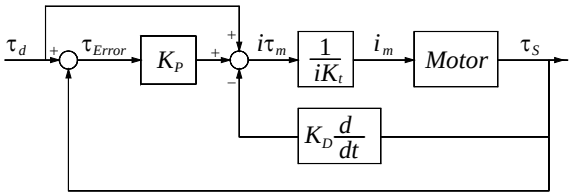

Fig. 14 Block diagram of PD torque control

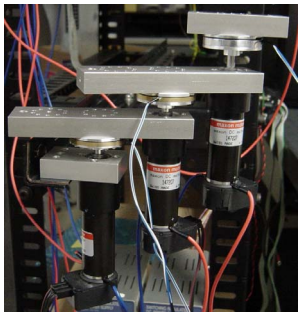

Fig. 15 Torque controlled links

4. CONCLUSION

New optical torque sensor has been developed using photointerrupter to measure the relative rotation. This invention allows realization of compact and light sensor. Besides, photointerrupter is easy to mount and replace, has a good linearity, enough resolution and does not affected by electromagnetic noise. New stage of research is realization of the local impedance control on the base of developed sensors.

5. REFERENCES

[1] Tadakuma, R., Kawabuchi, I., Kajimoto, H., Kawakami, N. and Tachi, S., "Mechanism of an Anthropomorphic 7-DOF Slave Arm for Telexistence," *Proceedings of 13th International Symposium on Measurement & Control in Robotics (ISMCR'03)*, Madrid, Spain, pp. 79-82, 2003.

[2] Tadakuma, R., Sogen, K., Kajimoto, H., Kawakami, N. and Tachi, S., "Development of Multi-D.O.F. Master-Slave Arm with Bilateral Impedance Control for Telexistence," *Proceedings of 14th International Symposium on Measurement & Control in Robotics (ISMCR'04)*, Houston, Texas, D21, 2004.

[3] S. Hirose and K. Yoneda, "Robotic sensors with photodetecting technology," *Proc. of 20th International Symposium on Industrial Robotics*, pp. 271-278, 1989.

[4] S. Hirose and K. Yoneda, "Development of optical 6-axial force sensor and its non-linear calibration," *J. of RSJ*, vol.8-25, pp.19-28, 1990.

[5] W. A. Lorenz, M. A. Peshkin, and J. E. Colgate, "New sensors for new applications: Force sensors for human/robot interaction," *Proc. of the 1999 IEEE International Conference on Robotics & Automation, Detroit, Michigan*, pp. 2855-2860, May 1999.

[6] N. Okutani and K. Nakazawa, "Torsion Angle Detection Apparatus and Torque Sensor," U. S. Patent 5 247 839, 1993.

[7] A. J. Hilton, "Force and Torque Converter," U. S. Patent 4 811 608, 1989.

[8] Photointerrupter Design Guide. *Product catalog of ROHM*, pp. 6-7, 2005.

[9] C. Nicot, "Torque Sensor for a Turning Shaft," U. S. Patent 6 694 828 B1, 2004.

[10] D. Vischer and O. Khatib, "Design and development of high-performance torque controlled joints," *IEEE Transactions on Robotic and Automation*, vol. 11, no. 4, pp. 537-544, August 1995.

[11] D. Vischer, O. Khatib, and J. Hake, "Joint torque sensory feedback in the control of PUMA manipulator," *IEEE Transactions on Robotic and Automation*, vol. 5, no. 4, pp. 418-425, August 1989.